

Posterior vitreous detachment and macular anatomical changes – a tomographic–electroretinographic study

ALIN-ȘTEFAN ȘTEFĂNESCU-DIMA¹⁾, CORNELIA ANDREEA CORÎCI²⁾, MARIA-RODICA MĂNESCU³⁾, TEODOR-NICUȘOR SAS⁴⁾, MARIA IANCĂU²⁾, CARMEN-LUMINIȚA MOCANU¹⁾

¹⁾Department of Ophthalmology, University of Medicine and Pharmacy of Craiova, Romania

²⁾Department of Physiology, University of Medicine and Pharmacy of Craiova, Romania

³⁾Department of Anatomy, University of Medicine and Pharmacy of Craiova, Romania

⁴⁾Department of Radiology and Imaging, University of Medicine and Pharmacy of Craiova, Romania

Abstract

Aim: Posterior vitreous detachment (PVD) is a physiological phenomenon due to aging characterized by separation of the vitreous cortex from the retina and may induce a variety of pathological events at the vitreoretinal junction. The aim of this study is to highlight *in vivo* anatomical and functional changes in early stages of PVD allowing the correct treatment. **Material and Methods:** Non-consecutive case series; optical coherence tomography (OCT) relies on analyzing the reflectivity of coherent light from different anatomical interfaces within posterior vitreous and retinal histological layers, thus acquiring transverse sections through vitreoretinal interface, sensory retina, retinal pigment epithelium and choroid. Modern techniques using Fourier spectral analysis of the reflected light enhance axial resolution to 5–10 μm, almost matching classic histological sections. Integrating these sections, OCT can reconstruct three-dimensional tissue anatomy. Full-field electroretinogram (ERG) evaluates the function of the entire retina evoked by a flash light. **Results:** Imaging of the vitreoretinal interface with OCT allowed staging PVD and correctly diagnosing its secondary pathologies: cystoid macular edema, vitreomacular traction syndrome, epiretinal membrane, macular pucker, macular hole, macular pseudohole, lamellar macular hole. The cone response of full-field ERG is a marker of retinal damage in macular pathology due to PVD. **Conclusions:** Correct understanding of vitreoretinal anatomic and functional changes due to posterior vitreous detachment is essential for a proper diagnosis and treatment.

Keywords: posterior vitreous detachment, vitreoretinal interface, OCT, electroretinogram.

Introduction

The vitreous, a highly hydrated transparent extracellular matrix, is the largest structure within the eye, constituting 80% of the ocular volume [1]. This structure is composed of two main portions: the central vitreous, and the cortical vitreous. The vitreous cortex is the outer lining of the vitreous and is attached to the internal limiting membrane (ILM) of the retina. The collagen fibers in the cortical vitreous are packed in a felt like network, in a direction parallel to the inner surface of the retina. The vitreous is most firmly attached to the vitreous base, but it is also strongly fixed to retinal vessels, optic nerve and macula.

The role of the vitreous in the physiology and pathobiology of the eye is being increasingly appreciated, but its anatomy is difficult to delineate *in vivo*, due to its invisible nature [1]. Even A. Vogt, thought observations in the posterior pole of the vitreous illusory rather than real [2].

Over time, the vitreous structure and anatomy were meticulously studied. Therefore, during the eighteen and nineteen centuries, the alveolar, lamellar, radial sector and fibrillar theories were formulated [3]. In 1814, Martegiani reported a funnel-shaped gel-free area immediately in front of the optic disc and this remnant of the primary hyaloid system [4] was named the space of Martegiani. In the early nineties, Baumann, Stroemberg & Redslob

considered these studies defective due to the use of tissue fixatives [3]. Biomicroscopic examination of the posterior gel was thought to empower clinical investigation, but it was severely compromised by bright, diffuse light reflected from the fundus and the low optical density of vitreous structure [4]. Also, this technique, spawned an equally varied set of descriptions of the vitreous: membranes, vertical and horizontal fibers arranged in intercrossing systems, grill-like pattern [3].

Studies using dark field microscopy and autopsy eyes dissected of sclera, choroid and retina suspended in a polymethyl methacrylate (PMMA) or Lucite chamber containing isotonic saline and sucrose, also brought various interpretations, ranging from fibrillar structure of the vitreous to “membranelles” in Eisner’s study [3]. Worst described the “tracts” of Eisner as constituting the walls of “cisterns” within the vitreous [3].

A larger gel-free “cisterna” located in front of the macula came to light in the 1970s and was named “bursa premacularis” [4].

The vitreous plays important roles for the entire eye, the main functions being mechanical, developmental, optical and metabolic. This highly hydrated gelatinous mass provides support to the retina, coordinates eye growth and brings metabolic nutrients requirements of the lens [5]. Nevertheless, the major function is to allow light to reach the retina, the vitreous transmitting 90% of light between 300 nm and 1400 nm [3].

In recent years, *in vivo* studies on vitreous anatomy were carried out through investigations such as optical coherence tomography (OCT) and ultrasonography. OCT provides an improved anatomic characterization of the cortical vitreous and vitreoretinal junction, allowing better insights into the vitreoretinal pathology. High-resolution OCT techniques, such as spectral or Fourier-domain OCT (FD-OCT), reveal all the retinal layers, as well as the vitreous and choroid, presented as a cross-section of the retina, which appears as a histological slice (Figure 1).

The main tool for assessing the function of the retina and vitreoretinal interface is the full-field electroretinogram (full-field ERG). The most important components of full-field ERG are the *a*-wave – representing the hyperpolarization of the photoreceptors in the outer retina [6], and the *b*-wave – reflecting the activity of the bipolar and Müller cells [6]. The ISCEV (*International Society for*

Clinical Electrophysiology of Vision) Standard ERG includes the following responses: dark-adapted 0.01 ERG (response to dim stimulation in dark adaptation, which evaluates rods response), dark-adapted 3.0 ERG (response to bright stimulus in dark adaptation, which analyses mixed rod-cone response), dark-adapted 3.0 oscillatory potentials ERG, light-adapted 3.0 ERG (response to a bright stimulus in light adaptation, which shows single flash cone response) and light-adapted 30 Hz flicker ERG (response to a flickering stimulus in light adaptation) [7].

One of the most important events in the life of the human vitreous [4] is the posterior vitreous detachment (PVD), defined as a dehiscence of the posterior hyaloid membrane (PHM) from internal limiting membrane (ILM) [8] in conjunction with vitreous liquefaction. PVD may induce a variety of pathological events at the vitreoretinal interface [9].

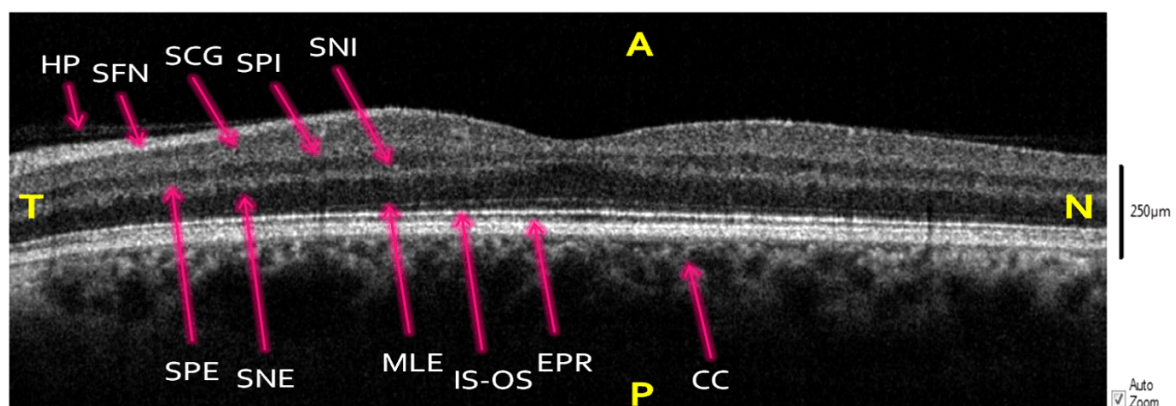


Figure 1 – Normal structure of the retina, emphasized through spectral-domain optical coherence tomography. *A*: Anterior; *P*: Posterior; *T*: Temporal; *N*: Nasal; *PH*: Posterior hyaloid; *NFL*: Nerve fiber layer; *GCL*: Ganglion cell layer; *IPL*: Inner plexiform layer; *INL*: Inner nuclear layer; *OPL*: Outer plexiform layer; *ONL*: Outer nuclear layer; *ELM*: External limiting membrane; *EZ*: Ellipsoid zone (inner/outer photoreceptor segment junction); *RPE*: Retinal pigment epithelium; *C*: Choroid.

Recent studies using OCT show that PVD begins in the perifoveal macula extend into the superior and temporal midperiphery, and then into the fovea, the inferior midperiphery and finally the optic disc margin, resulting in complete PVD [9].

In OCT assessment, the vitreoretinal separation was classified in stages. Accordingly to Stanga *et al.*, stage 0 indicated no PVD; stage 1 was characterized by focal perifoveal PVD, limited to either the temporal or nasal side of the fovea, with persistent attachment to the fovea and optic nerve head; stage 2, focal perifoveal PVD, involving both the temporal and nasal side of the fovea, with persistent attachment to the fovea and optic nerve head; stage 3, PVD over the fovea with persistent attachment to the optic nerve head; stage 4 complete PVD over the macula and optic nerve head; stage 5, PVD not gradable [4].

Vitreous separation may go unnoticed by the patient, and clinically undetected, until separation from the optic disc margin produces symptoms like floaters and an arc of golden or white light in the temporal field of vision [10] and signs of a Weiss ring.

Using imaging methods, like high-resolution optical coherence tomography, is essential in understanding pathogenesis, evolution and in detecting complications of early and late-stage PVD.

The aim of our study is to highlight the anatomic *in vivo* and functional changes in early stages of PVD, using OCT and full-field ERG, allowing in time and correct treatment.

☒ Patients, Materials and Methods

This is a retrospective non-consecutive study, conducted according to the tenets of the Declaration of Helsinki. All patients were informed about this study and gave their informed consent to being imaged and for the collected data to be used for publication.

One hundred patients attending our Clinic for the spectral-domain OCT were considered for the study. Patients with diabetic maculopathy, retinal vein occlusion, age-related macular degeneration, high and medium myopia, history of retinal detachment and macular edema were excluded. Therefore, 10 patients who met the inclusion–exclusion criteria described above were included into the study.

OCT scans were performed in our Department, using spectral-domain optical coherence tomography systems (TOPCON 3D OCT-2000 and OPTOVUE IVUE). These systems operate at a scanning speed of 40000 A-scans/second using a wavelength of 850 nm and an axial resolution of 7 μm.

For each patient, the attached/detached PHM, the integrity of vitreoretinal interface, the architecture of the retinal layers, the central macular thickness, the integrity of inner segment/outer segment (IS/OS) junction were assessed.

ERGs were recorded using MonPackOne System (Metrovision, Perenchies, France). Recording electrodes were HK loop type (“Hawlina–Konec loop”) and the reference and ground ones were Ag–AgCl cup type.

Results

We present 10 non-consecutive cases with vitreoretinal junction pathology, clinically visible or not, but very well highlighted through spectral-domain optical coherence tomography (SD-OCT). The electroretinographic changes are variable, depending on the degree of retinal damage.

Case No. 1 is a 61-year-old male with a normal aspect of the fundus. On the OCT image, it can be seen that the posterior hyaloid membrane is detached in the nasal and temporal quadrant and attached in the foveal region, with an empty space in the premacular region, suggesting stage 2 PVD and bursa premacularis (Figure 2).

Case No. 2 is a 78-year-old female patient who clinically presents a yellow macular ring. OCT shows detachment of the PHM nasally, in both horizontal and vertical sections, with tractional effect on the inner layers of the retina, intraretinal cystoid spaces within the outer nuclear layer, full thickness macular hole, disruption of IS/OS junction and normal retinal pigment epithelium (RPE), suggesting stage 2 PVD and stage 3 macular hole (MH) (Figure 3).

Case No. 3 is a 75-year-old male patient with a clinically seen yellow ring. OCT shows detachment of the PHM nasally and temporally, with persisting foveal attachment seen on the vertical section, full thickness macular hole (FTMH) with subretinal fluid, disruption of the IS/OS suggesting stage 2 PVD and stage 3 MH (Figure 4).

Case No. 4 is a 69-year-old female showing abnormal retinal light reflex with mild retinal thickening and a foveal dark spot. The SD-OCT shows a complete detachment of the PHM, a hyper-reflective line above ILM with retinal folds suggesting epiretinal membrane (ERM) with

contractile effect. There is also a stage 4 MH with sub-retinal fluid and disruption of IS/OS (Figure 5).

Case No. 5 is a 69-year-old female with a fundoscopic aspect of macular dark spot. The SD-OCT shows a completely detached PHM, a break in the inner fovea with intact foveal photoreceptors, decreased central macular thickness, but normal perifoveal retinal thickness. This aspect is highly suggestive of stage 4 PVD and lamellar macular hole (Figure 6).

Case No. 6 shows a 79-year-old female patient whose OCT shows a completely detached PHM, hyper-reflective layer on the surface of the retina with retinal folds but globally adherent, intraretinal cyst in the macular region and normal architecture of the outer layers. The retinal map reveals increased macular thickness (Figure 7).

Case No. 7 is a 66-year-old female with absence of foveal light reflex and a small foveal red spot. The OCT reveals a complete detachment of the PHM with a break in the inner fovea with intact foveal photoreceptors and near-normal retinal thickness, suggesting stage 4 PVD and lamellar macular hole (Figure 8).

Case No. 8 is a 63-year-old patient with an abnormal retinal light reflex, irregular wrinkling of the inner retina and a foveal red spot on funduscopy. The SD-OCT shows hyper-reflective line above the surface of the retina with retinal folds, intraretinal cyst, dehiscence of inner from outer retinal layers, macular hole, small neuroepithelium detachment with intact IS/OS (Figure 9).

Case No. 9 is a 66-year-old patient presenting a translucent membrane with abnormal retinal light reflex. SD-OCT shows hyper-reflective layer on the surface of the retina with underlying corrugation of the retinal surface and blunting of the foveal contour and normal architecture of the outer retina. Retinal map shows increased retinal thickness (Figure 10).

Case No. 10 is a 37-year-old female, post-vitrectomy after a traumatic posteriorly luxated lens, which clinically shows irregular pigmentary changes in the central macular region. SD-OCT reveals attached retina with atrophy of the foveal layers and a highly decreased retinal thickness (Figure 11).

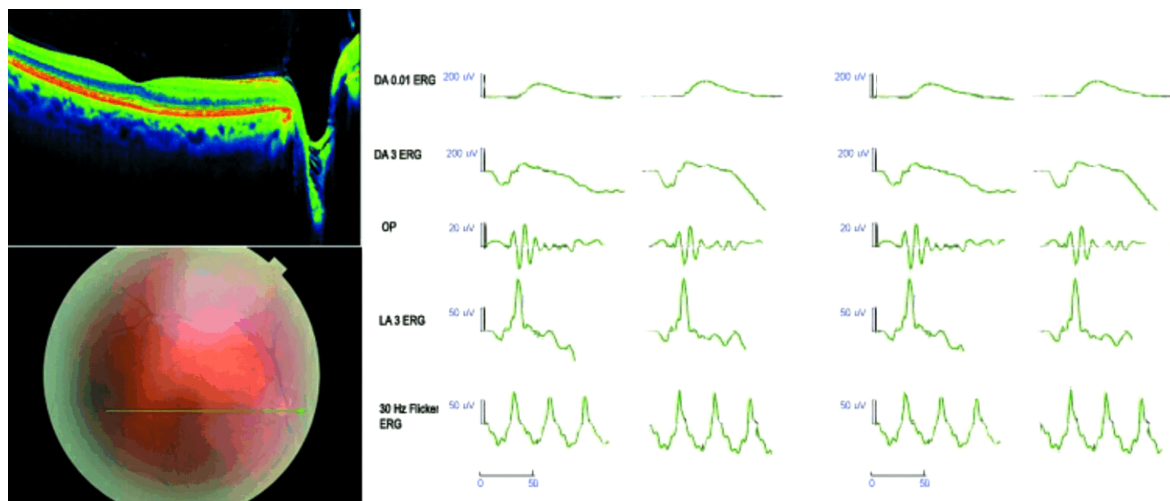


Figure 2 – Normal aspect of the fundus while the OCT shows a stage 2 PVD and the presence of bursa premacularis. Full-field ERG is normal (compared to a normal subject).

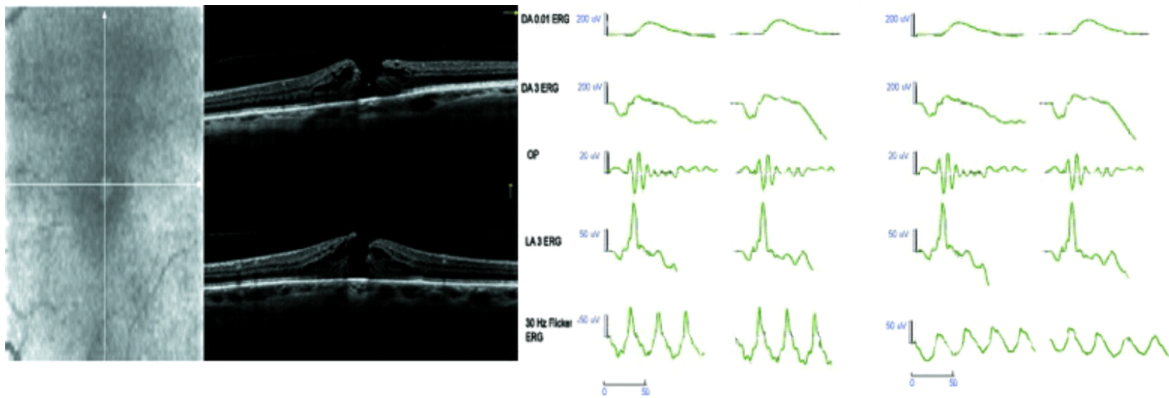


Figure 3 – Red free photo showing macular dark spot and SD-OCT showing stage 2 PVD and stage 3 MH. Full-field ERG shows decreased and delayed 30 Hz Flicker (compared to a normal subject).

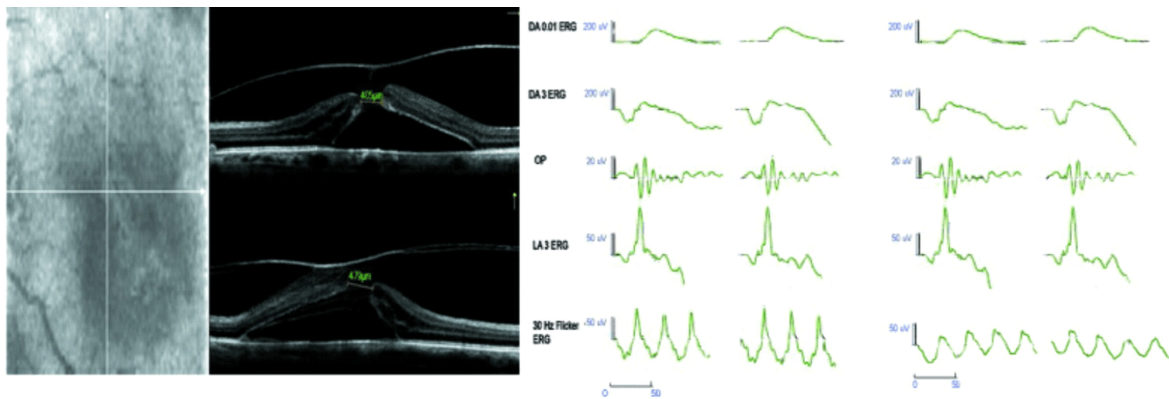


Figure 4 – Red free photo showing a macular dark spot. SD-OCT showing stage 2 PVD and stage 3 MH. Full-field ERG shows decreased and delayed 30 Hz Flicker.

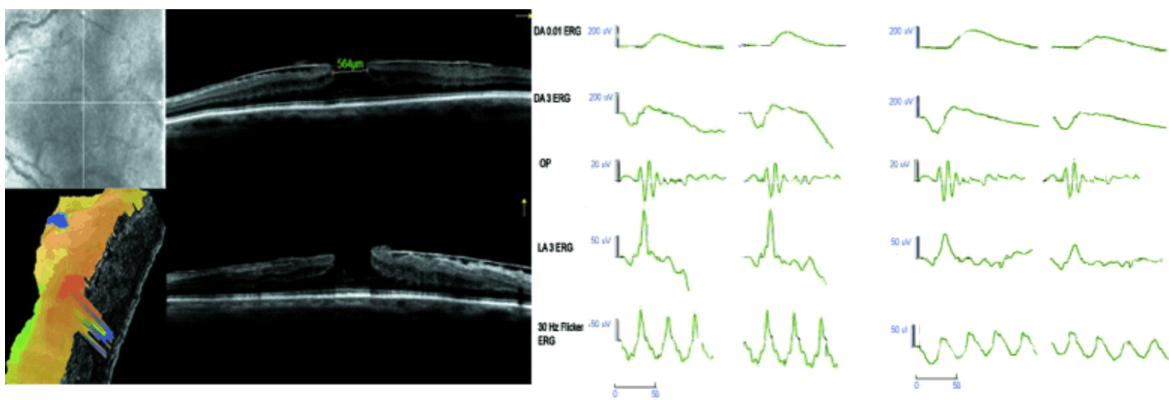


Figure 5 – Red free photo showing a macular translucent membrane with a foveal dark spot. SD-OCT showing stage 4 PVD, stage 4 MH, ERM with tractional retinal effect. Full-field ERG shows decreased LA (low amplitude) 3 b-wave and decreased and delayed 30 Hz Flicker.

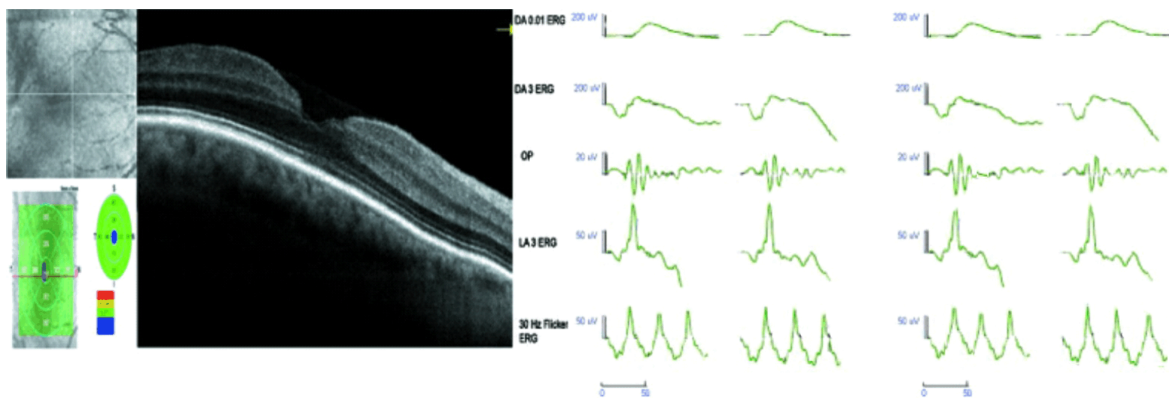


Figure 6 – Red free photo showing absence of the foveal reflex SD-OCT showing stage 4 PVD and lamellar MH. Decreased central macular thickness (CMT) and normal perifoveal retinal thickness. Normal full-field ERG.

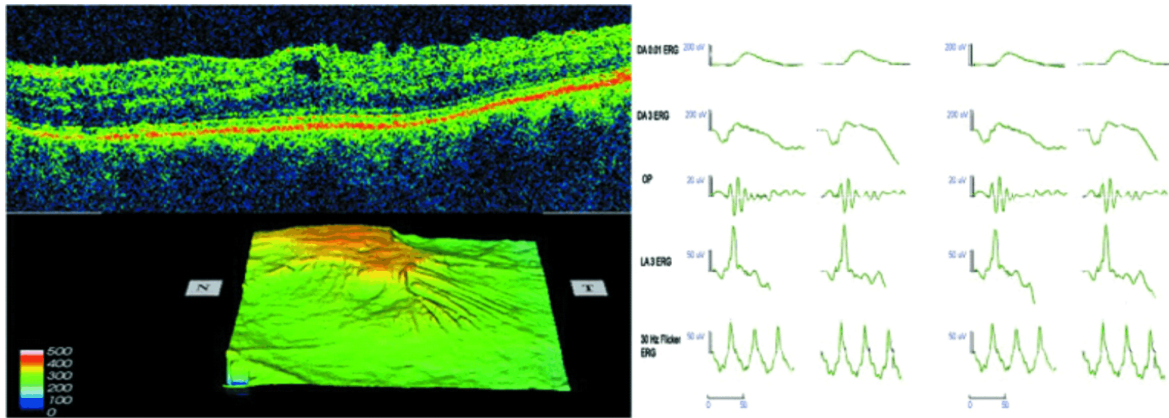


Figure 7 – SD-OCT showing foveal pseudocyst (stage 1 MH), stage 4 PVD and ERM. Retinal map shows increased CMT. Normal full-field ERG.

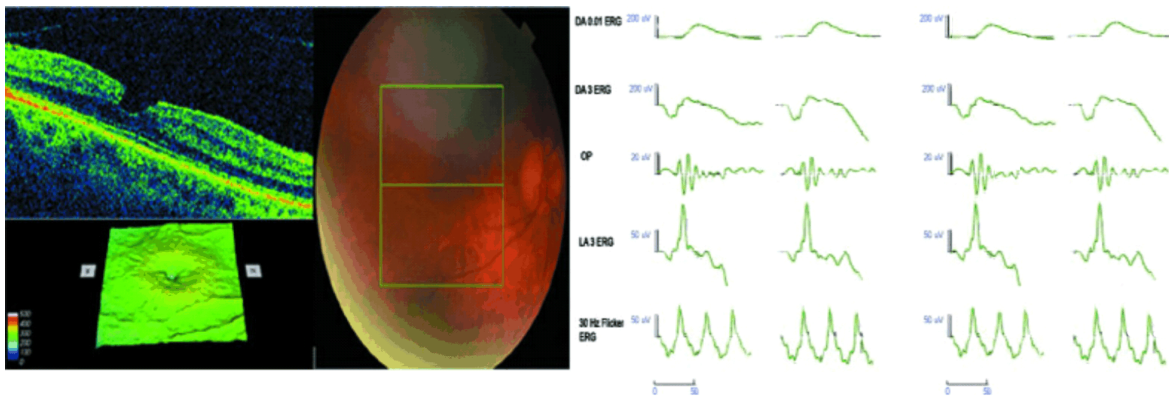


Figure 8 – Fundus photo showing absence of foveal light reflex with small foveal red spot. SD-OCT showing stage 4 PVD and lamellar MH. Retinal map showing near-normal retinal thickness. Normal full-field ERG.

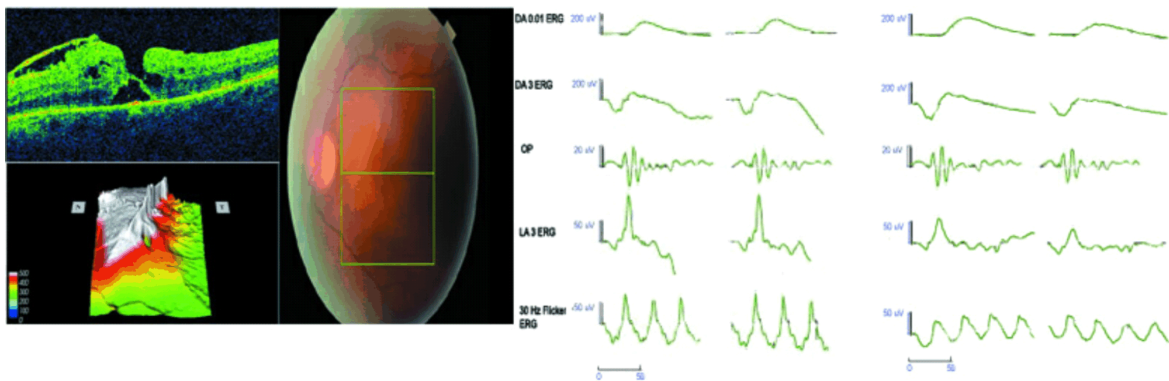


Figure 9 – Fundus photo showing abnormal retinal light reflex with a foveal red spot. SD-OCT showing ERM with tractional retinal effect, intraretinal split, MH stage, subretinal fluid. Retinal map shows increased thickness. Full-field ERG shows decreased LA 3 b-wave and decreased and delayed 30 Hz Flicker.

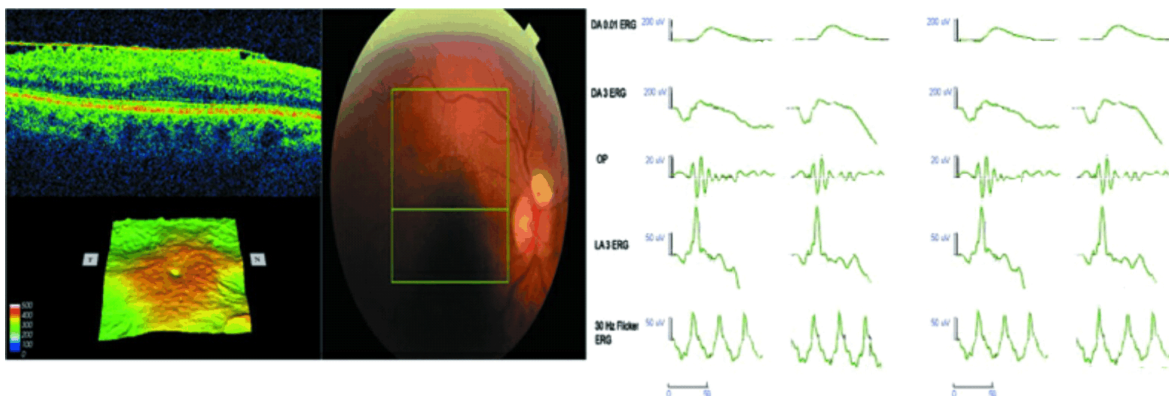


Figure 10 – Fundus photo showing an epiretinal translucent membrane. SD-OCT showing epiretinal membrane with tractional retinal effect. Retinal map showing increased CMT. Normal full-field ERG.

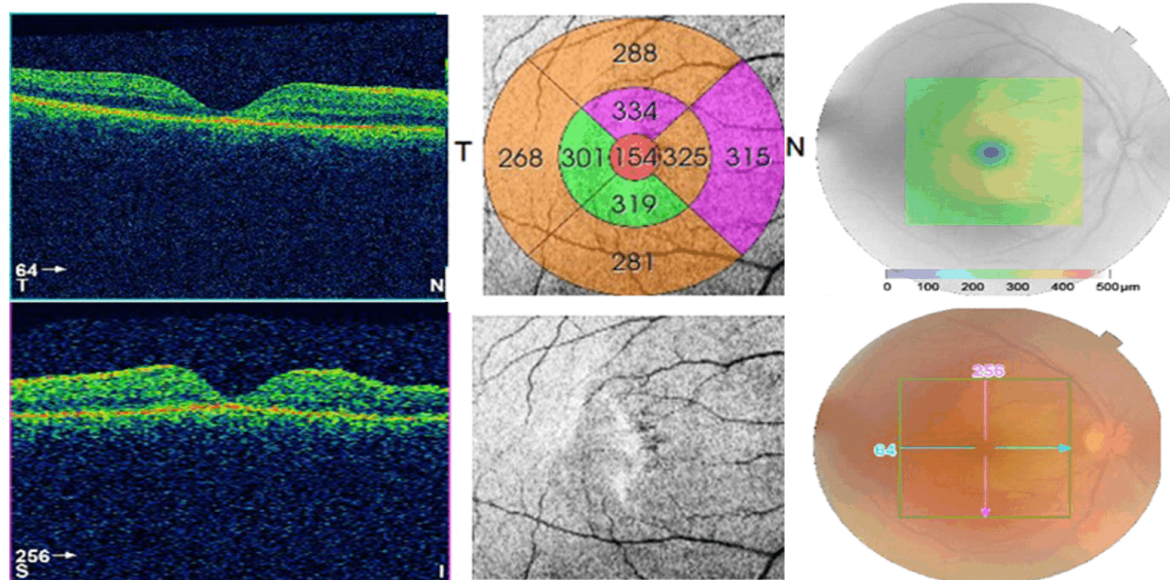


Figure 11 – Fundus photo, red free photo and OCT in a post-vitrectomy patient. *T*: Temporal; *N*: Nasal; *S*: Superior; *I*: Inferior.

Discussion

The vitreous, the gel which fills the centre of the eye, occupying 80% of the ocular volume, is a structure that was very much studied over time. Even so, its anatomy, morphology and function are not fully elucidated. Its complex and incompletely understood involvement in the health of the eye, still is a topic of great interest for both clinicians and scientists.

Starting with the eighteenth century, multiple techniques for vitreous study, like: freezing and slowing thawing, dissection and histological preparation with tissue fixatives, *ex vivo* and *in vivo* slit-lamp biomicroscopy, dark field microscopy, were used [3]. After dissecting the gel from its scleral, choroidal and retinal vestments, Sebag & Balazs, suspended the vitreous in a PMMA chamber and used slit-beam biomicroscopy to confirm points of structural weakness in the posterior cortical vitreous [4], bursa pre-macularis and space of Martegiani.

Over the last 25 years, imaging of the eye has grown significantly in importance for the ocular disease diagnosis [11]. Besides techniques such as: scanning laser polarimetry, scanning laser ophthalmoscopy, optical coherence tomography has emerged to the forefront of ocular imaging due to its high resolution and the complex three-dimensional data that is able to gather [11].

The first image of retinal disease were produced in 1995 showing both the foveal contour and optic nerve head *in vivo*, using time-domain OCT [12]. However, there was relatively low imaging speed, motion artifacts and relatively poor sensitivity and resolution [12].

A major advance was the development of spectral or Fourier-domain OCT that enables much faster acquisition times, resulting in a large increase in the amount of data that can be obtained during a given scan duration [11]. SD-OCT is of particular utility in investigating retinal, vitreoretinal and vitreous normal and pathological morphology.

At the boundary between physiological and pathological, posterior vitreous detachment is the culmination of aging changes in the vitreous and may induce a variety

of pathological events at the vitreoretinal interface [9], such as: epimacular membrane, macular microhole, idiopathic macular hole, inner lamellar hole, vitreo-foveolar traction, vitreomacular traction syndrome, retinal hemorrhage, vitreous hemorrhage, retinal tear, rhegmatogenous retinal detachment [9]. According to PVD staging, these complications can be divided into early- and late-stage complications.

Bursa pre-macularis

Bursa pre-macularis, also known as posterior precortical vitreous pocket (PPVP) [4], was described by Worst, in 1970, and confirmed by Sebag & Balazs, through dark field microscopy. It is a point of structural vulnerability in the pre-macular cortical vitreous, usually seen in individuals <65 years old [4].

Highlighting bursa pre-macularis through biomicroscopy is almost impossible owing to vitreous transparency and moving. Using SD-OCT, the presence of PPVP can be well observed and measured (Figure 2). Through the high scanning speed and axial resolution, a three-dimensional image of the posterior vitreous and vitreoretinal interface can be obtained, visualizing anatomical structures, such as bursa pre-macularis.

In other studies, Mojana *et al.* detected the posterior vitreous in 89% of 202 eyes and the prevalence of bursa pre-macularis in 42% of all cases, using SD-OCT [13]. Itakura observed the presence of PPVP in 83.3% of 102 eyes using FD-OCT and in 100% using an even newer OCT technique – swept-source OCT. Stanga *et al.* found a prevalence of bursa pre-macularis in 57.1% of 238 eyes (119 patients) [4].

Therefore, bursa pre-macularis is an anatomical item of the posterior pre-macular vitreous, whose existence was discovered through dark field microscopy and that can now be highlighted through OCT.

Epiretinal membrane

Epiretinal membrane (ERM) consists of an avascular layer of cells that form and overlie the macula [14]. The

development of ERM involves glial cells, retinal pigment epithelium cells, macrophages, fibrocytes and collagen fibers [15]. Epiretinal membrane can be idiopathic or it can be associated with posterior vitreous detachment, retinal breaks, vascular retinopathy, ocular inflammation, congenital ocular disorders, laser photocoagulation or retinal detachment surgery [15]. There are several hypotheses on epiretinal membrane formation. One of these supports the fact that vitreoretinal traction during the development of PVD may cause dehiscence in the inner limiting membrane through which glial cells can migrate and proliferate on the inner retinal surface [9]. Another assumption is that ERM may result from the proliferation and transdifferentiation of hyalocytes contained within vitreous cortical remnants left on the retinal surface after PVD [9].

Epiretinal membrane can be asymptomatic or it can contract leading to metamorphopsia, distorted and blurred central vision. Regarding the diagnosis, ERM can be detected on clinical fundus examination, but the certainty diagnosis, the characteristics of the membrane and also the surgical indication and postoperative visual outcome are assessed through optical coherence tomography.

OCT features of epiretinal membrane are: hyper-reflective line above ILM with or without retinal folds showing the contractile or non-contractile effect on retina, increased central macular thickness (CMT), macular edema, effect on IS/OS junction. Macular edema and IS/OS junction defect are associated with long-term disease and thus increase damage to photoreceptor cells and worsened functionality [15].

In our study, four patients were found with PVD and ERM. In large clinical studies, PVD was found in 80% to 100% of eyes with ERM, showing a high correlation between these two entities [9]. It is considered that eyes previously reported as having no PVD, actually had early stages of PVD that could not be discerned clinically [9].

Idiopathic or full thickness macular hole

Idiopathic or full thickness macular hole (FTMH) is characterized by a full thickness neuroretinal break or defect of the macula, affecting the inner and outer retinal layer and leads to visual impairment [16]. In many cases, is related to posterior vitreous detachment and is mainly seen in elderly [17].

The pathogenesis of macular hole' formation is still unclear, but it is broadly believed to have a strong relationship with the vitreous traction exerted on the fovea [17]. Therefore, anatomical changes such as intraretinal split, foveal pseudocyst and foveolar detachment have been described as the primary findings in the macular hole' development. The presence of intraretinal cysts may be an indicator of ILM traction, which may activate Müller cells and cause accumulation of extracellular fluid in the retina [18].

It has been generally accepted that anteroposterior vitreous traction on the foveola exerted by a posterior hyaloid membrane results in fovea splits or pseudo cysts formation and rarely fovea detachment [19–21]. Pseudocysts formation has extended posterior, disrupting the outer photoreceptor layer and vitreous traction has led to the opening of the inner roof of the cyst, with development of a full thickness MH [19–22].

A fovea pseudocyst must be one of the next stages of inner fovea splits in the process that may be a part of the continuum of full thickness MH formation [21]. In some cases, a fovea pseudocyst opens without disruption of the outer retinal layer, resulting in a partial thickness MH or lamellar hole that may not progress to a full thickness MH [21, 23, 24].

The features of the MH are very important for the surgical indications, and especially for postoperative visual outcome. The diameter of the MH and the base diameter, which can only be measured by OCT, seem to represent prognostic factors, as it reflects the real size of the retinal lesion [23].

Spectral-domain OCT provides *in vivo* high-resolution cross-sectional images of the microstructure of retinal tissue. It has been used to characterize idiopathic macular hole in order to understand its morphology, staging and pathogenesis.

Total retinal function, explored through full-field ERG, has been evaluated in a few studies on patients with macular hole. In a study on 19 patients, Andréasson & Ghosh found a delayed cone implicit time, showing that the entire retinal function is affected [25]. They also made a correlation between the full-field ERG and the visual outcome after macular hole' surgery, demonstrating a change in the cone response 18 months after surgery [25].

In our study, we found four patients with FTMH. All four patients presented changes in full-field ERG, the most sensitive being the 30 Hz Flicker.

Conclusions

OCT imaging of the foveal anatomy and vitreoretinal interface refined our understanding of the natural history of PVD and improved etiological diagnosis in several related conditions: cystoid macular edema, vitreomacular traction syndrome, epimacular membrane, macular hole, macular pseudohole, macular lamellar hole, etc. In macular pathology, cone response of full-field ERG may be of great interest in evaluating the retinal function.

Conflict of interests

The authors declare that they have no conflict of interests.

References

- [1] de Smet MD, Gad Elkareem AM, Zwinderman AH. The vitreous, the retinal interface in ocular health and disease. *Ophthalmologica*, 2013, 230(4):165–178.
- [2] Hruby K. Clinical examination of the vitreous body. *Proc R Soc Med*, 1954, 47(3):163–170.
- [3] Sebag J. The vitreous: structure, function, and pathobiology. Springer-Verlag, New York, 1989, 80–95.
- [4] Stanga PE, Sala-Puigdollers A, Caputo S, Jaberansari H, Cien M, Gray J, D'Souza Y, Charles SJ, Biswas S, Henson DB, McLeod D. *In vivo* imaging of cortical vitreous using 1050-nm swept-source deep range imaging optical coherence tomography. *Am J Ophthalmol*, 2014, 157(2):397–404.e2.
- [5] Murthy KR, Goel R, Subbannayya Y, Jacob HK, Murthy PR, Manda SS, Patil AH, Sharma R, Sahasrabudde NA, Parashar A, Nair BG, Krishna V, Prasad TsK, Gowda H, Pandey A. Proteomic analysis of human vitreous humor. *Clin Proteomics*, 2014, 11(1):29.
- [6] Graham SL, Klistorner A. Electrophysiology: a review of signal origins and applications to investigating glaucoma. *Aust N Z J Ophthalmol*, 1998, 26(1):71–85.

- [7] Marmor MF, Fulton AB, Holder GE, Miyake Y, Brigell M, Bach M; International Society for Clinical Electrophysiology of Vision. ISCEV Standard for full-field clinical electroretinography (2008 update). *Doc Ophthalmol*, 2009, 118(1):69–77.
- [8] Ivastinovic D, Schwab C, Borkenstein A, Lackner EM, Wedrich A, Velikay-Parel M. Evolution of early changes at the vitreo-retinal interface after cataract surgery determined by optical coherence tomography and ultrasonography. *Am J Ophthalmol*, 2012, 153(4):705–709.
- [9] Johnson MW. Posterior vitreous detachment: evolution and complications of its early stages. *Am J Ophthalmol*, 2010, 149(3):371–382.e1.
- [10] Snead MP, Snead DR, James S, Richards AJ. Clinico-pathological changes at the vitreo-retinal junction: posterior vitreous detachment. *Eye (Lond)*, 2008, 22(10):1257–1262.
- [11] Schuman JS. Spectral domain optical coherence tomography for glaucoma (an AOS thesis). *Trans Am Ophthalmol Soc*, 2008, 106:426–458.
- [12] Sebag J. *Vitreous in health and disease*. Springer-Verlag, Science + Business Media, New York, 2014.
- [13] Mojana F, Kozak I, Oster SF, Cheng L, Bartsch DU, Brar M, Yuson RM, Freeman WR. Observations by spectral-domain optical coherence tomography combined with simultaneous scanning laser ophthalmoscopy: imaging of the vitreous. *Am J Ophthalmol*, 2010, 149(4):641–650.
- [14] Mason JO 3rd, Patel SA. Efficacy of vitrectomy and epiretinal membrane peeling in eyes with dry age-related macular degeneration. *Clin Ophthalmol*, 2015, 9:1999–2003.
- [15] Pavlidis M, Georgalas I, Körber N. Determination of a new parameter, elevated epiretinal membrane, by *en face* OCT as a prognostic factor for *pars plana* vitrectomy and safer epiretinal membrane peeling. *J Ophthalmol*, 2015, 2015:838646.
- [16] Duan HT, Chen S, Wang YX, Kong JH, Dong M. Visual function and vision-related quality of life after vitrectomy for idiopathic macular hole: a 12mo follow-up study. *Int J Ophthalmol*, 2015, 8(4):764–769.
- [17] Harasawa M, Quiroz-Mercado H, Salcedo-Villanueva G, Garcia-Aguirre G, Schwartz S. Inner segment ellipsoid band and cone outer segment tips changes preceding macular hole development in a young patient. *Case Rep Ophthalmol Med*, 2014, 2014:132565.
- [18] Chen H, Chen W, Zheng K, Peng K, Xia H, Zhu L. Prediction of spontaneous closure of traumatic macular hole with spectral domain optical coherence tomography. *Sci Rep*, 2015, 5:12343.
- [19] Gaudric A, Haouchine B, Massin P, Paques M, Blain P, Erginay A. Macular hole formation: new data provided by optical coherence tomography. *Arch Ophthalmol*, 1999, 117(6):744–751.
- [20] Kishi S, Takahashi H. Three-dimensional observations of developing macular holes. *Am J Ophthalmol*, 2000, 130(1):65–75.
- [21] Haouchine B, Massin P, Gaudric A. Foveal pseudocyst as the first step in macular hole formation: a prospective study by optical coherence tomography. *Ophthalmology*, 2001, 108(1):15–22.
- [22] Ullrich S, Haritoglou C, Gass C, Schaumberger M, Ulbig MW, Kampik A. Macular hole size as a prognostic factor in macular hole surgery. *Br J Ophthalmol*, 2002, 86(4):390–393.
- [23] Takahashi A, Yoshida A, Nagaoka T, Kagokawa H, Kato Y, Takamiya A, Sato E, Yokota H, Ishiko S, Hirokawa H. Macular hole formation in fellow eyes with a perifoveal posterior vitreous detachment of patients with a unilateral macular hole. *Am J Ophthalmol*, 2011, 151(6):981–989.e4.
- [24] Yeh PT, Chen TC, Yang CH, Ho TC, Chen MS, Huang JS, Yang CM. Formation of idiopathic macular hole-reappraisal. *Graefes Arch Clin Exp Ophthalmol*, 2010, 248(6):793–798.
- [25] Andréasson S, Ghosh F. Cone implicit time as a predictor of visual outcome in macular hole surgery. *Graefes Arch Clin Exp Ophthalmol*, 2014, 252(12):1903–1909.

Corresponding author

Cornelia Andreea Corici, MD, PhD Student, Department of Physiology, University of Medicine and Pharmacy of Craiova, 2 Petru Rareș Street, 200349 Craiova, Dolj County, Romania; Phone +40766–212 416, e-mail: corici.andreea@gmail.com

Received: November 9, 2015

Accepted: August 26, 2016